Capture cross sections from (p,d) reactions

J.E. Escher[1,a], J.T. Burke[1], R.J. Casperson[1], R.O. Hughes[1], S. Ota[2], and N.D. Scielzo[1]

[1] Lawrence Livermore National Laboratory, Livermore, CA 94550, USA
[2] Texas A&M University, College Station, TX 77843, USA

Abstract. Cross sections for compound-nuclear reactions involving unstable targets are important for many applications, but can often not be measured directly. Several indirect methods have been proposed to determine neutron capture cross sections for unstable isotopes. We consider an approach that aims at constraining statistical calculations of capture cross sections with data obtained from light-ion transfer reactions such as (p,d). We discuss the theoretical descriptions that have to be developed in order to extract meaningful cross section constraints from such data and show some benchmark results.

1. Introduction

Neutron-capture reactions on unstable isotopes are of interest to astrophysics and other applications [1,2]. Cross sections for many short-lived isotopes have to be calculated, but suffer from large uncertainties due to poorly-constrained inputs. Several indirect methods are currently being explored for their ability to provide constraints for these calculations: The compound nuclei (CN) of interest are produced via light-ion inelastic scattering and transfer reactions, photon-induced reactions, and nuclear β decay [3–6] and constraints come from measurements of the subsequent CN decay. Each method has strengths, as well as experimental and theoretical challenges that have to be overcome in order to provide reliable capture cross sections for nucleosynthesis modeling and other applications. In particular, the formation of the CN in the indirect approach has to be understood in order to correct for differences between the measured and desired reactions.

This contribution discusses the example of one-nucleon transfer reactions. The procedure for obtaining constraints on neutron capture calculations is explained, the theoretical methods needed to describe (p,d) transfer reactions that result in a CN are outlined, and a comparison with experimental observables is shown.

2. Cross section calculations and constraints from indirect measurements

The CN capture reaction $n + A \rightarrow B^* \rightarrow \gamma + B$ is described in the statistical Hauser-Feshbach formalism [7,8], which accounts for conservation of angular momentum and parity:

$$\sigma_{n+A,\chi}(E_n) = \sum_{J,\pi} \sigma^{CN}_{n+A}(E_{ex}, J, \pi)\ G^{CN}_{\chi}(E_{ex}, J, \pi)\ . \quad (1)$$

Here $\chi = \gamma + B$ denotes the exit channel, and the excitation energy E_{ex} of B^* is related to the neutron energy via $E_n = \frac{A+1}{A}(E_{ex} - S_n)$, where S_n is the neutron separation energy of the nucleus B. Width fluctuation corrections have been omitted here, but have to be included in the calculations. The CN formation cross section, $\sigma^{CN}_{n+A} = \sigma(n + A \rightarrow B^*)$, can be calculated using existing optical potentials. The theoretical decay probabilities G^{CN}_{χ} for the different decay channels χ are often quite uncertain, since they contain transmission coefficients, $T^J_{\chi ls}$, for all competing exit channels, the associated level densities, $\rho_I(U)$, in the various residual nuclei, as well as information on discrete levels:

$$G^{CN}_{\chi}(E_{ex}, J, \pi) = \frac{\sum_{\ell s I} \int T^J_{\chi \ell s} \rho_I(U) dE_{\chi}}{\sum'_{\chi' \ell' s'} T^J_{\chi' \ell' s'} + \sum_{\chi' \ell' s' I'} \int T^J_{\chi' \ell' s'}(E_{\chi'}) \rho_{I'}(U') dE_{\chi'}}\ . \quad (2)$$

The quantities ℓ and ℓ' are the relative orbital angular momenta in the exit channels and $\rho_I(U)$ is the density of levels of spin I at energy U in the residual nucleus. The denominator includes contributions from decays to discrete levels and to regions described by a level density. All sums over quantum numbers must respect parity conservation, although this is not explicitly expressed here.

Much effort has been devoted to develop models to calculate nuclear level densities and transmission coefficients for particles, photons, and fission, and to formulate parameter recommendations [9]. Auxiliary experiments provide important constraints for these models and their parameters. Most notably, neutron resonance measurements provide average level spacings and thus constraints for the level densities near the neutron separation energy [10]. Average radiative widths provide information on the product of the level density and the γ-ray strength function.

For reactions involving unstable targets, the requisite neutron resonance spacings and average radiative capture widths are not available, and the decay probabilities $G^{CN}_{\chi}(E_{ex}, J, \pi)$ become the primary source of uncertainty in calculations of capture cross sections. Evaluations

[a] e-mail: escher1@llnl.gov

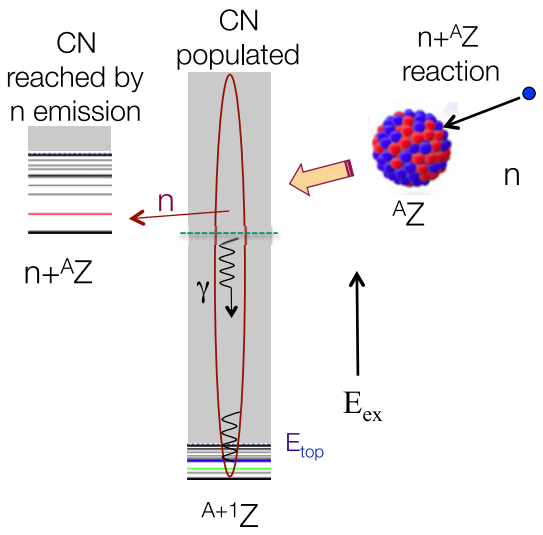

Figure 1. Schematic of a capture reaction. In a compound neutron capture process, the neutron and target nucleus ^{A}Z fuse to form the compound nucleus $^{A+1}$Z, which subsequently decays via a γ-ray cascade. This occurs in competition with neutron emission (shown) and other decays (not indicated).

typically rely on regional systematics in this case, and a factor two (or more) difference between evaluated cross sections is not uncommon; for reactions involving nuclei far from stability the uncertainties increase to more than an order of magnitude. It is the purpose of indirect methods to provide constraints that reduce the uncertainties in the calculated cross sections. For the reactions of interest here, the indirect approaches produce the relevant CN and obtain useful information from observing its decay.

In an approach that has become known as the 'surrogate method' [3], the compound nucleus B^* is produced by an inelastic scattering or transfer reaction $d + D \rightarrow b + B^*$ (Fig. 2), and the desired decay channel is observed in coincidence with the outgoing particle b at angle θ_b. The probability for forming $B^* = {}^{A+1}Z^*$ in the surrogate reaction (with specific values for E_{ex}, J, π) is $F_\delta^{CN}(E_{ex}, J, \pi, \theta_b)$, where δ refers to the surrogate reaction $D(d, b)$. The quantity

$$P_{\delta\chi}(E_{ex}, \theta_b) = \sum_{J,\pi} F_\delta^{CN}(E_{ex}, J, \pi, \theta_b)\ G_\chi^{CN}(E_{ex}, J, \pi)\ , \tag{3}$$

which gives the probability that the CN B^* was formed with energy E_{ex} and decayed into channel χ, can be obtained experimentally by detecting a discrete γ-ray transition characteristic of the residual nucleus (or some other suitable observable).

The distribution $F_\delta^{CN}(E_{ex}, J, \pi, \theta_b)$, which may be very different from the CN spin-parity populations following the absorption of a neutron in the desired reaction, has to be determined theoretically, so that the branching ratios $G_\chi^{CN}(E_{ex}, J, \pi)$ can be extracted from the measurements. In practice, the decay of the CN is modeled using a Hauser-Feshbach-type decay model and the $G_\chi^{CN}(E_{ex}, J, \pi)$ are obtained by adjusting parameters in the model to reproduce the measured probabilities $P_{\delta\chi}(E_{ex}, \theta_b)$. Subsequently, the sought-after cross section can be obtained by combining the calculated cross section $\sigma_\alpha^{CN}(E_{ex}, J, \pi)$ for the formation of

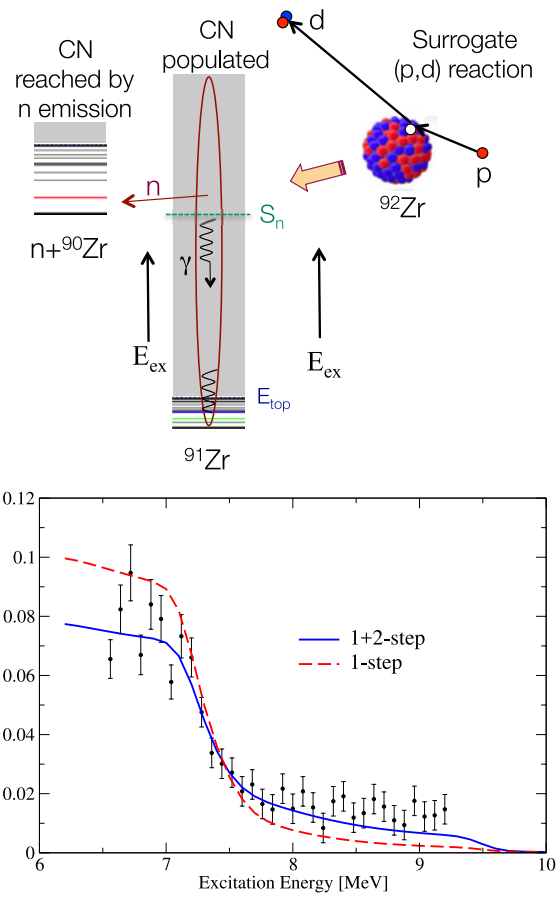

Figure 2. CN formation and decay in a surrogate transfer reaction. Top panel: The CN ^{91}Zr* is produced via the ^{92}Zr(p,d)^{91}Zr reaction and subsequently decays via neutron evaporation and γ emission. Characteristic γ-ray transitions in ^{91}Zr are measured in coincidence with the outgoing deuteron. Bottom panel: Measured coincidence probability for the decay of ^{91}Zr. The probability of observing the 1466 keV ($5/2^+ \rightarrow 5/2^+$) transition in coincidence with the outgoing deuteron is given as function of E_{ex} (black data points with error bars). The curves show predicted coincidence probabilities based on one-step (dashed curve) and two-step (solid curve) calculations. These results are preliminary.

$B^* = {}^{A+1}Z^*$ (from n+^{A}Z) with the extracted decay probabilities $G_\chi^{CN}(E_{ex}, J, \pi)$ for this state, see Eq. (1).

The problem with previous attempts of obtaining (n,γ) cross sections from surrogate measurements has been that the surrogate spin-parity populations $F_\delta^{CN}(E_{ex}, J, \pi, \theta_b)$ were not available and approximations had to be introduced. Typically, it was assumed that either the decay probabilities $G_\chi^{CN}(E_{ex}, J, \pi)$ are independent of spin and parity or that the surrogate and desired reactions populate the CN in a similar manner. Both theoretical [11–13] and experimental investigations [14–17] have demonstrated that these assumptions are not valid.

3. Surrogate (p,d) reactions: Theory and experimental tests

Generating accurate predictions of the surrogate spin-parity (J^π) distribution is challenging, as it requires a model for the reaction mechanisms that are involved in the formation of the compound nucleus. Here we consider the example of ^{92}Zr(p,d)^{91}Zr* which produces the CN ^{91}Zr*.

This CN is relevant to the ^{90}Zr(n,γ) reaction, for which much information (resonance spacings, average radiative width, cross section) is known; this case thus serves as illustrative example and useful test case.

In the example considered here, the surrogate reaction produces ^{91}Zr* by removing neutrons from inner shells of the ^{92}Zr nucleus: $2p_{1/2}$, $2p_{3/2}$, $1f_{5/2}$, $1f_{7/2}$, etc., hole states are involved in the production of ^{91}Zr* near S_n. Their location and fragmentation as a function of E_{ex} was obtained using the dispersive optical model approach of Mahaux and Sartor [18]. At the high excitation energies involved, one-step (p,d) pickup processes have to be complemented by contributions from two-step processes such as (p,p')(p',d) and (p,d')(d',d), in which the initial ^{92}Zr or the final ^{91}Zr are inelastically excited. The calculations were carried out using the coupled-channels code FRESCO [19]. The proton-nucleus optical potential by Koning and Delaroche [20] was used to describe the entrance channel, and the deuteron-nucleus potential by Daehnick et al. [21] was employed for the exit channel.

Due to the large number of states in the energy band populated, the different contributions can be assumed to add incoherently. The weights $F_\delta^{CN}(E_{ex}, J, \pi, \theta_b)$ of the final spins can then be determined from the relative contributions of the individual cross sections to the total (p,d) cross section.

To test the theoretical description of this process, one can compare the total (p,d) cross section to the measured cross section. The dispersive optical model, which gives energy-averaged quantities, is not expected to reproduce the details of the rich nuclear structure present at low excitation energies ($E_{ex} \lesssim$ 2–3 MeV). At higher energies ($E_{ex} \approx$3–10 MeV) the combination of dispersive optical model and two-step approach is found to be in reasonable agreement with the measurements [22]. Observables that are very sensitive to the details of the spin distribution of the CN prior to decay are individual γ-ray transitions in ^{91}Zr. The present case involves stable nuclei for which information on levels, level densities, and γ-ray strength functions is available, so the γ-cascade can be modeled and tests of the theory predicting the CN population $F_\delta^{CN}(E_{ex}, J, \pi, \theta_b)$ can be carried out. This is, of course, opposite to the planned procedure of determining an unknown cross section by adjusting the decay model to reproduce the surrogate data, but it allows us to test the description.

The requisite experiment was carried out at the Texas A&M University Cyclotron Institute, where the K150 Cyclotron was employed to provide a 28.5-MeV proton beam. Particle-γ coincidence data was collected using the STARLiTeR array, a combination of a silicon telescope array and five HPGe clover detectors [23]. The outgoing deuteron was detected at angles around 30°–60° and γ-rays for transitions between low-lying states ($E_n <$ 2 MeV) were measured.

In the bottom panel of Fig. 2 the predicted surrogate probabilities $P_{\delta\chi}^{theo}(E_{ex})$ are compared to this data. Here we show the coincidence probability for the 1466 keV transition (from the $5/2^+$ state at 1.466 MeV to the $5/2^+$ ground state) as a function of E_{ex} in ^{91}Zr. When the CN ^{91}Zr is populated below the neutron threshold (S_n = 7.19 MeV), less than 10% of the decays proceed through this transition. As the excitation energy is increased beyond S_n, neutron emission begins to compete and the γ-probability drops quickly. The solid and dashed curves are the results of calculations that combine predictions for the weights $F_\delta^{CN}(E_{ex}, J, \pi, \theta_b)$ in Eq. (3) with a Hauser-Feshbach-type decay model for ^{91}Zr. The calculated spin distributions $F_\delta^{CN}(E_{ex}, J, \pi, \theta_b)$ were integrated over the experimental angular range, and $P_{\delta\chi}^{theo}(E_{ex})$ refers to the associated angle-integrated probability.

Good agreement is found for the full 1+2-step calculation (solid curve) while the 1-step calculation (dashed curve) fails to reproduce the 'shoulder' above about 7.5 MeV. Similar shape differences are found for other transitions (not shown).

This comparison illustrates that the two-step contributions play an important role in the reaction: The 1-step removal of a neutron from the ^{92}Zr nucleus produces excited states in ^{91}Zr with angular momentum of at most $J = 9/2$ (by removal from the $1g_{9/2}$ orbital), with $J = 3/2^-$ and $J = 5/2^-$ (*i.e.*, removal from the $1f_{3/2}$ and $1f_{5/2}$ orbitals) dominating the distribution near the neutron separation energy. Two-step reactions, proceeding via inelastic $L = 1^-, 2^+, \ldots, 8^+$, on the other hand, produce spin distributions that contain contributions up to $J = 25/2$, with the dominant contributions near S_n coming from $J = 3/2$ to $J = 9/2$. The coupling of inelastic excitations and neutron removal, which leads to final states with large J values, is found to be critical for reproducing the measured coincidence probabilities.

4. Conclusions

We outlined a procedure for obtaining constraints for calculations of neutron capture cross sections using observables from experiments with transfer reactions. To illustrate the idea, we discussed preliminary results from a (p,d) experiment in the Zr region. The decay of compound nuclei in this region is known to be particularly sensitive to the spins and parities populated via a surrogate reaction [11,12,14,23,24]. We demonstrated that the light-ion reaction can be sufficiently well described to reproduce the indirect measurement observables. This is a first step towards extracting the desired cross section from the indirect data. An application of the method to obtain an unknown cross section for capture on a neighboring unstable isotope is underway [22].

An advantage of using inelastic scattering and transfer reactions to produce the CN of interest lies in the variety of projectile-target combinations that can be utilized. That makes it possible to reach a large number of isotopes, in particular when the technique can be combined with radioactive beams in inverse-kinematics experiments [25,26].

Current investigations focus mostly on isotopes close to stability, where benchmarking is facilitated by the availability of auxiliary information and, in some cases, directly-measured cross sections. The longer-term goal is to develop methods that can be used for a wider range of reactions. Radioactive beams are now available at multiple facilities. The availability of these exotic beams makes it possible to produce important isotopes using inelastic scattering and transfer reactions in inverse kinematics, as well as via β-decay, and to study of the subsequent competition between neutron and γ-ray emission.

We thank the Operations and Facilities staff at the Texas A&M University Cyclotron Institute for support during the experiment.

This work was performed under the auspices of the U.S. Department of Energy (DOE) by Lawrence Livermore National Laboratory under contract DE-AC52-07NA27344, with partial support through LLNL's LDRD (16-ERD-022) and ASC/PEM programs.

References

[1] A. Arcones, D.W. Bardayan, T.C. Beers, L.A. Bernstein, J.C. Blackmon, B. Messer, B.A. Brown, E.F. Brown, C.R. Brune, A.E. Champagne et al., Progress in Particle and Nuclear Physics (2016)

[2] Nuclear Science Advisory Committee, *Reaching for the Horizon: The 2015 Long Range Plan for Nuclear Science* (2015)

[3] J.E. Escher, J.T. Burke, F.S. Dietrich, N.D. Scielzo, I.J. Thompson, W. Younes, Rev. Mod. Phys. **84**, 353 (2012)

[4] R. Raut, A.P. Tonchev, G. Rusev, W. Tornow, C. Iliadis, M. Lugaro, J. Buntain, S. Goriely, J.H. Kelley, R. Schwengner et al., Phys. Rev. Lett. **111**, 112501 (2013)

[5] A. Spyrou, S.N. Liddick, A.C. Larsen, M. Guttormsen, K. Cooper, A.C. Dombos, D.J. Morrissey, F. Naqvi, G. Perdikakis, S.J. Quinn et al., Phys. Rev. Lett. **113**, 232502 (2014)

[6] S.N. Liddick, A. Spyrou, B.P. Crider, F. Naqvi, A.C. Larsen, M. Guttormsen, M. Mumpower, R. Surman, G. Perdikakis, D.L. Bleuel et al., Phys. Rev. Lett. **116**, 242502 (2016)

[7] W. Hauser, H. Feshbach, Phys. Rev. **87**, 366 (1952)

[8] P. Fröbrich, R. Lipperheide, *Theory of Nuclear Reactions* (Clarendon Press, Oxford, 1996)

[9] R. Capote, M. Herman, P. Oblozinský, P. Young, S. Goriely, T. Belgya, A. Ignatyuk, A. Koning, S. Hilaire, V. Plujko et al., Nuclear Data Sheets **110**, 3107 (2009)

[10] S.F. Mughabghab, *Atlas of Neutron Resonances, Resonance Parameters and Thermal Cross Sections* $Z = 1 - 100$, 5th edn. (Elsevier, Amsterdam, 2006)

[11] C. Forssén, F. Dietrich, J. Escher, R. Hoffman, K. Kelley, Phys. Rev. C **75**, 055807 (2007)

[12] J.E. Escher, F.S. Dietrich, Phys. Rev. C **81**, 024612 (2010)

[13] S. Chiba, O. Iwamoto, Phys. Rev. C **81**, 044604 (2010)

[14] N.D. Scielzo, J.E. Escher, J.M. Allmond, M.S. Basunia, C.W. Beausang, L.A. Bernstein, D.L. Bleuel, J.T. Burke, R.M. Clark, F.S. Dietrich et al., Phys. Rev. C **81**, 034608 (2010)

[15] R. Hatarik, L.A. Bernstein, J.A. Cizewski, D.L. Bleuel, J.T. Burke, J.E. Escher, J. Gibelin, B.L. Goldblum, A.M. Hatarik, S.R. Lesher et al., Phys. Rev. C **81**, 011602 (2010)

[16] G. Boutoux, B. Jurado, V. Méot, O. Roig, L. Mathieu, M. Aïche, G. Barreau, N. Capellan, I. Companis, S. Czajkowski et al., Physics Letters B **712**, 319 (2012)

[17] Q. Ducasse, B. Jurado, M. Aïche, P. Marini, L. Mathieu, A. Görgen, M. Guttormsen, A.C. Larsen, T. Tornyi, J.N. Wilson et al., Phys. Rev. C **94**, 024614 (2016)

[18] C. Mahaux, R. Sartor, in *Advances in nuclear physics* (Springer US, 1991), Vol. 20, pp. 1–223

[19] I.J. Thompson, Computer Physics Reports **7**, 167 (1988)

[20] A.J. Koning, J.P. Delaroche, Nucl. Phys. **A713**, 231 (2003)

[21] W.W. Daehnick, J.D. Childs, Z. Vrcelj, Phys. Rev. C **21**, 2253 (1980)

[22] J.E. Escher et al. (2017), to be published

[23] S. Ota, J.T. Burke, R.J. Casperson, J.E. Escher, R.O. Hughes, J.J. Ressler, N.D. Scielzo, I.J. Thompson, R.A.E. Austin, B. Abromeit et al., Phys. Rev. C **92**, 054603 (2015)

[24] S. Ota, J. Burke, R. Casperson, J. Escher, R. Hughes, J. Ressler, N. Scielzo, I. Thompson, R. Austin, E. McCleskey et al., EPJ Web of Conferences **93**, 02001 (2015)

[25] J. Cizewski, R. Hatarik, K. Jones, S. Pain, J. Thomas, M. Johnson, D. Bardayan, J. Blackmon, M. Smith, R. Kozub, Nuclear Instruments and Methods in Physics Research Section B: Beam Interactions with Materials and Atoms **261**, 938 (2007)

[26] A. Ratkiewicz, J. Cizewski, S. Pain, A. Adekola, J. Burke, R. Casperson, N. Fotiades, M. McCleskey, S. Burcher, C. Shand et al., EPJ Web of Conferences **93**, 02012 (2015)